RevMexAA (Serie de Conferencias), **36**, CD312–CD318 (2009)

SIMULATIONS AND ANALYSIS OF THE POLARISED RADIO SKY

J. Geisbuesch[1] and P. Alexander[1]

RESUMEN

Presentamos simulaciones del cielo en radio polarizado a las longitudes de onda del Square Kilometre Array (SKA). Se discuten como algunas mediciones de polarización lineal pueden ser utilizadas para explorar propiedades de la polarización intrínsecas a las fuentes, así como para estudiar los campos magnéticos en cúmulos de galaxias mediante la rotación de Faraday. Para este propósito consideramos modelos de fuentes y cúmulos de diferente grado de complejidad. Hacemos predicciones para el SKA. Usando métodos Bayesianos de análisis estadístico, encontramos límites a las propiedades de la polarización de las fuentes y de los campos magnéticos de los cúmulos.

ABSTRACT

We present simulations of the polarised radio sky at Square Kilometre Array (SKA) wavebands. Further, we discuss how measurements of linear polarisation can be used to explore intrinsic source polarisation properties and to study the magnetic fields of galaxy clusters via Faraday rotation of the polarisation plane. For this purpose, we consider source and cluster models of differing complexity. We make forecasts for the SKA. By applying Bayesian statistical analysis methods, we quantify constraints which can be placed on source polarisation properties and cluster magnetic fields.

Key Words: galaxies: clusters — galaxies: magnetic fields — galaxies: spiral — magnetic fields — techniques: polarimetry

1. INTRODUCTION

A powerful tool for studying magnetic fields in a variety of environments is to use Faraday rotation against background polarised sources. This population of sources consists mainly of star-forming galaxies and different types of radio AGN. In order to analyse spectral polarisation data, we need to have a (most general) parameterised model for the background source population. The model must allow for structure of polarised emission in the source together with intrinsic depolarisation. Between the emitting source and the observer, we must consider not only the average Faraday depth on the accessible resolution scale, but also depolarisation due to angular structures in Faraday (foreground) screens on scales smaller than the telescope resolution or the angular size of the illuminating source respectively. Moreover, bandwidth effects have to be taken into account. However, given the resolution, sensitivity and bandwidth of the proposed SKA (see Schilizzi et al. 2007 for the latest design specifications of the SKA), which are expected to be achieved by baselines of up to thousands of kilometres, a total collection area at its final stage of more than 10^6 square metres and an ultra-wide band coverage of the antennas with high simultaneous channel number outputs, future SKA observations are expected to be much less affected by spatial and frequency resolution and thus depolarisation issues than it is the case for present polarisation studies. In particular, for continuum studies the completed instrument is expected to reach sub-arcsecond resolution in the frequency range most interesting for polarisation studies (from ~ 300 MHz to ~ 5 GHz), an instantaneous channel read-out of $\gtrsim 400$ MHz and observational flux limits which are for reasonable integration times dominated by Galactic foregrounds and source confusion rather then instrumental noise properties.

2. MODELLING POLARISED SOURCES

To obtain realistic models of radio source populations, we use the publically available SKADS (Wilman et al. 2008) synthetic radio source catalogue (S^3). The catalogue is derived from semi-empirical simulations of different populations of radio continuum sources and extends down to faint flux limits in order to allow observation simulations of high-sensitive future radio facilities, such as the SKA and the Low Frequency Array (LOFAR). The source populations included in the catalogue are radio-loud (FRI and FRII) and radio-quiet AGNs as well as radio emitting starburst and normal disk galaxies. These populations are of utmost importance, if not

[1]Astrophysics Group, Cavendish Laboratory, University of Cambridge, UK (joern@mrao.cam.ac.uk).

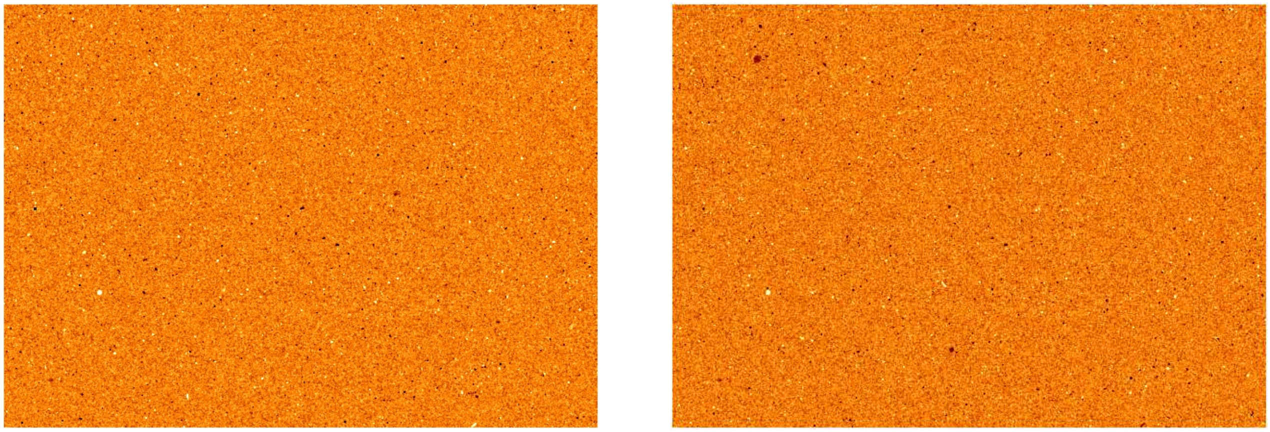

Fig. 1. Sky simulation of linearly polarised sources. The Stokes parameters Q (left panel) and U (right panel) are shown.

constituting a complete list of radio emitting source types in the considered observing frequency range and flux regimes. The luminosity function corresponding to each class of sources is derived empirically from available observations. The fits are extrapolated to low luminosities and assume redshift evolutions to assure the simulations are complete down to the instrumentally expected (faint) flux limits.

To determine the degree of polarisation of individual sources, we employ two different approaches. The first, an empirical and statistical one, is based on current radio source surveys with polarisation information available; e.g. our modelling makes use of polarisation statistics obtained from the NVSS catalogue (Condon et al. 1998). For example, Tucci et al. 2003 have analysed polarisation statistics from the NVSS and other sources in great detail. Depending on spectral shape and source flux, they derived median fractional polarisations between 1.12% and 1.77% for NVSS sources. Explicitly, we model the probability distribution of fractional source polarisations by a log-normal function which fits the observed 1.4 GHz function at the high fractional polarisation tail. Moreover, in this approach we adopt the depolarisation correction suggested by Tucci et al. (2003) to obtain the intrinsic source polarisation and use 10 GHz as a reference frequency since Faraday depolarisation is expected to be of minor importance if not negligible at frequencies $\nu \gtrsim 10$ GHz. A simulated polarised sky in the Stokes parameters Q and U obtained by applying this approach is shown in Figure 1.

Another way to generate a polarised sky simulation is to create analytic or numerical models for each type of source population present in the radio continuum. A polarised sky can then be obtained from these models in combination with provided number counts by Monte Carlo simulations (by placing certain priors on the model parameters). For example, it is expected that a large number –if not even the vast majority– of polarised sources detectable by SKA observations will be spiral star-forming (and starburst) galaxies. Their magnetic field consists of a disk and a much weaker halo component apart from a random turbulent component. Dependent on the origin of the seed magnetic field and mode excitation, disks mainly possess axis- and/or bisymmetric regular dynamo fields. However, sometimes even higher excitation modes, such as quadrisymmetric ones, are observed in superposition to the "standard" ones (see e.g. Beck et al. 1996 for a review). The fractional contribution of the poloidal halo field component is often found to increase radially and with distance from the disk, while the absolute toroidal component amplitude decreases away from the disk. The turbulent component arises from stellar activity, merging and all sorts of turbulent flow motions induced, for example, by shocks during structure formation due to material accretion and infall. Its magnitude is generally of the order of the regular field one.

Figure 2 shows the degree of polarisation of the over the galactic disk integrated radio synchrotron emission of normal galaxies with different geometries of the regular toroidal component of the galactic magnetic field for a fixed disk inclination with respect to the line-of-sight and different ratios of the regular to random field components. Moreover, in Figure 3 the integrated polarisation degree is plotted for different inclinations of galaxies with the same regular field geometry and slope of the random field

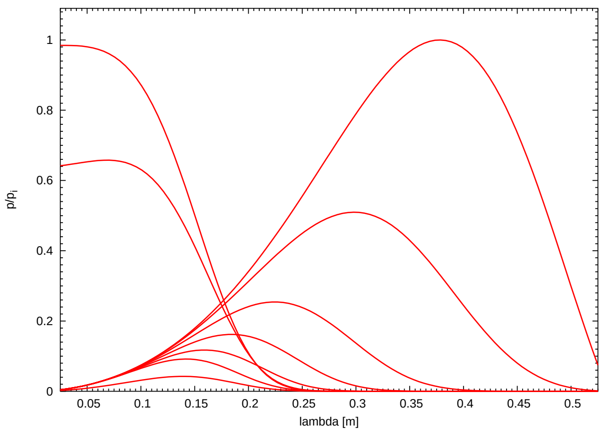

Fig. 2. The degree of polarisation for different models of normal galaxies with respect to observing frequency. The differences in these analytic model predictions result from assumptions made about the particular galaxy regular field geometries and the amplitude of random turbulent field contributions.

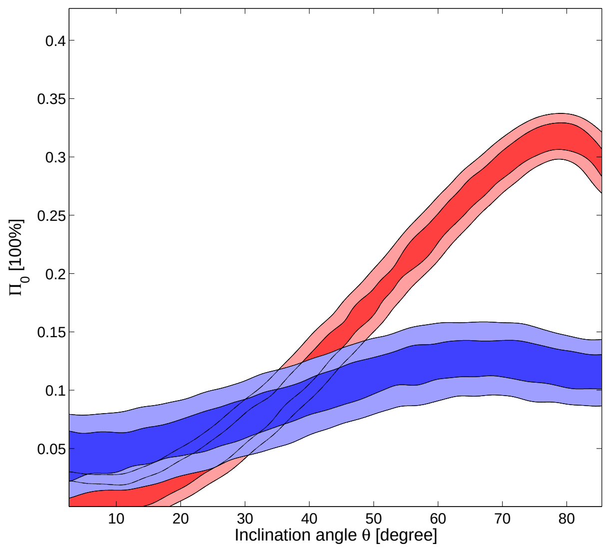

Fig. 3. The integrated polarisation fraction, Π_0, for different model galaxies as function of inclination. The shown likelihood contours of the integrated polarisation fraction have been obtained in each case by Monte Carlo simulations. The contours give the 68.3% and 95.4% likelihoods that a model spiral galaxy with a given inclination has a specific integrated polarisation fraction. Red contours: A model with a low random field component in comparison to the regular field. Blue contours: A model with a realistic random field component whose amplitude is comparable to the regular field one.

power spectrum, though, different *rms* amplitudes of the random field realisation at a fixed observing frequency. The scatter at a constant inclination is due to Monte Carlo realisations of the turbulent random field.

3. CLUSTERS AS FARADAY FOREGROUND SCREENS

Common magnetic field strengths in clusters are typically $0.1 - 1$ μG. Cooling flow clusters have stronger magnetic fields than non-cooling flow clusters – up to an order of magnitude stronger. Radio images of clusters show halos and relics, which suggest that wide-spread magnetic fields reside in clusters (minimum energy calculations give $B \sim 0.4 - 1$ μG).

3.1. *Modelling cluster magnetic fields*

The observational data on the structure of magnetic fields in clusters is presently rather sparse. Thus, we employ at first a rather simple model for their rotation measure structure. Our model of the rotation measure (RM) cluster profile has a central peak value which is either drawn from a distribution or obtained by a scaling and its radial decline is given by a King model ($\mathrm{RM}(r) = \mathrm{RM}_0 \left(1 + (r/r_c)^2\right)^{-3\beta/2}$). In particular, we make the choice of $\beta = 1$ in order to approximate the resulting RM profile for a gas density distribution with $\beta = 2/3$ in an isothermal cluster. Moreover, the central cluster magnetic field strength and electron density can be obtained empirically from observations or by physically motivated scalings with other known cluster properties, thus yielding the central cluster RM amplitude. To model the cluster number and distribution within an observed patch of sky, we employ N-body simulations. This approach ensures that the spatial correlation of clusters is correctly modelled. Using this modelling approach the RM distribution due to galaxy clusters in a typical survey field can be obtained. A realisation is shown in the left panel of Figure 4. Our simulations compare statistically well with observations.

A more advanced way to model cluster magnetic fields is to divide up the cluster into cells on whose scale the electron density and magnetic field vector can be regarded as uniform. To model correlations of cell magnetic field vectors, we assume a power law spectrum. For the electron density distribution we adopt again a conventional King profile and also scale the magnetic field strength in a similar fashion (i.e. decreasing with cluster radius). Figure 5 shows cluster magnetic field realisations for different assumed spectral indices, n, of the cluster magnetic field power spectrum. The larger n is, the less power

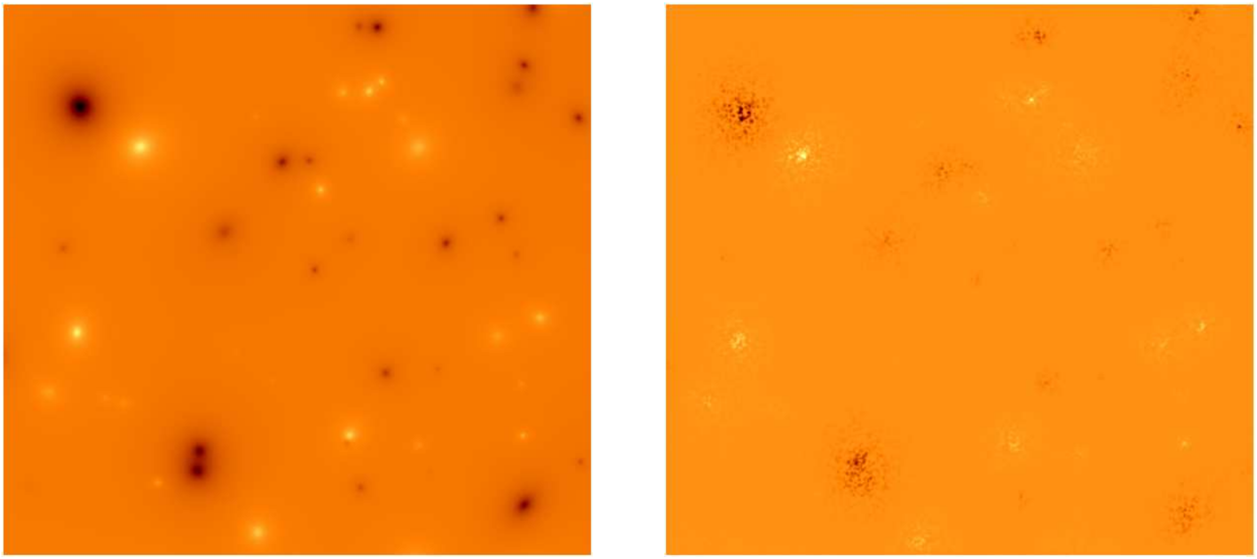

Fig. 4. RM simulation (left panel) and sampling by a source grid (right panel).

resides in small scale fluctuations. Figure 6 shows how the Faraday depth changes along different lines of sight through a cluster.

4. ROTATION MEASURE GRIDS

Cluster X-ray or SZ data in combination with RM observations can yield an estimate of cluster magnetic fields. However, current RM grids are sparse and the sample of clusters which have a larger number of polarisation measurements of imbedded or background sources is small. The SKA with its unique collection area will reach unmatched sensitivities in reasonable integration times. Thus, the number of source detections within a cluster will significantly increase. Especially, the increase in the number of background sources will be of the order of several magnitudes compared to current wide field surveys (e.g. NVSS). Note that integration times might in some wavebands even be source confusion limited (dependent on cosmology, radio source properties and their evolution). In the right panel of Figure 4 we plot the sampling of the RM distribution by polarised sources for a reasonably deep SKA observation. Further discussion of (SKA) RM grids is given in Geisbuesch et al. 2008 and Alexander et al. 2008.

5. RECONSTRUCTING FARADAY AND POLARISATION PROPERTIES

To investigate the potential of future SKA data to determine (radio) source intrinsic and (cluster) foreground screen magneto-ionic properties, we model SKA mid band observations based on the most recent SKA reference design (see Schilizzi et al. 2007). Our line-of-sight simulations assume a population of high redshift background radio sources which are "Faraday shadowed" by medium redshift foreground galaxy clusters. Our mock background source population is modelled to agree with recent observations. In particular, the source modelling has been adjusted so that the resulting degrees of polarisation are consistent with observed Stokes I, Q and U, and RM data of such sources. The spectral behaviours of their polarisation degrees are governed by source internal magneto-ionic structures causing source intrinsic Faraday rotations of the polarisation plane. While high redshift sources can be considered as roughly point-like unresolved objects, turbulent magnetic field structures imbedded in foreground clusters' thermal electron atmospheres are expected to vary mainly on scales larger than the assumed SKA resolution. Moreover, the smallest spatial scales of considerable turbulent field fluctuations in clusters are estimated to be larger than the area illuminated by a common high redshift background source, so that beam depolarisation should be close to negligible and the cluster magnetic field (well) resolvable (see e.g. Murgia et al. 2004). For generating mock data for our analysis we assume telescope integration times of approximately 3 hours. Furthermore, at present the modelling does not include Galactic foregrounds and Earth atmospheric disturbances.

To the simulated data, we apply a Bayesian RM synthesis analysis, which uses a Markov Chain

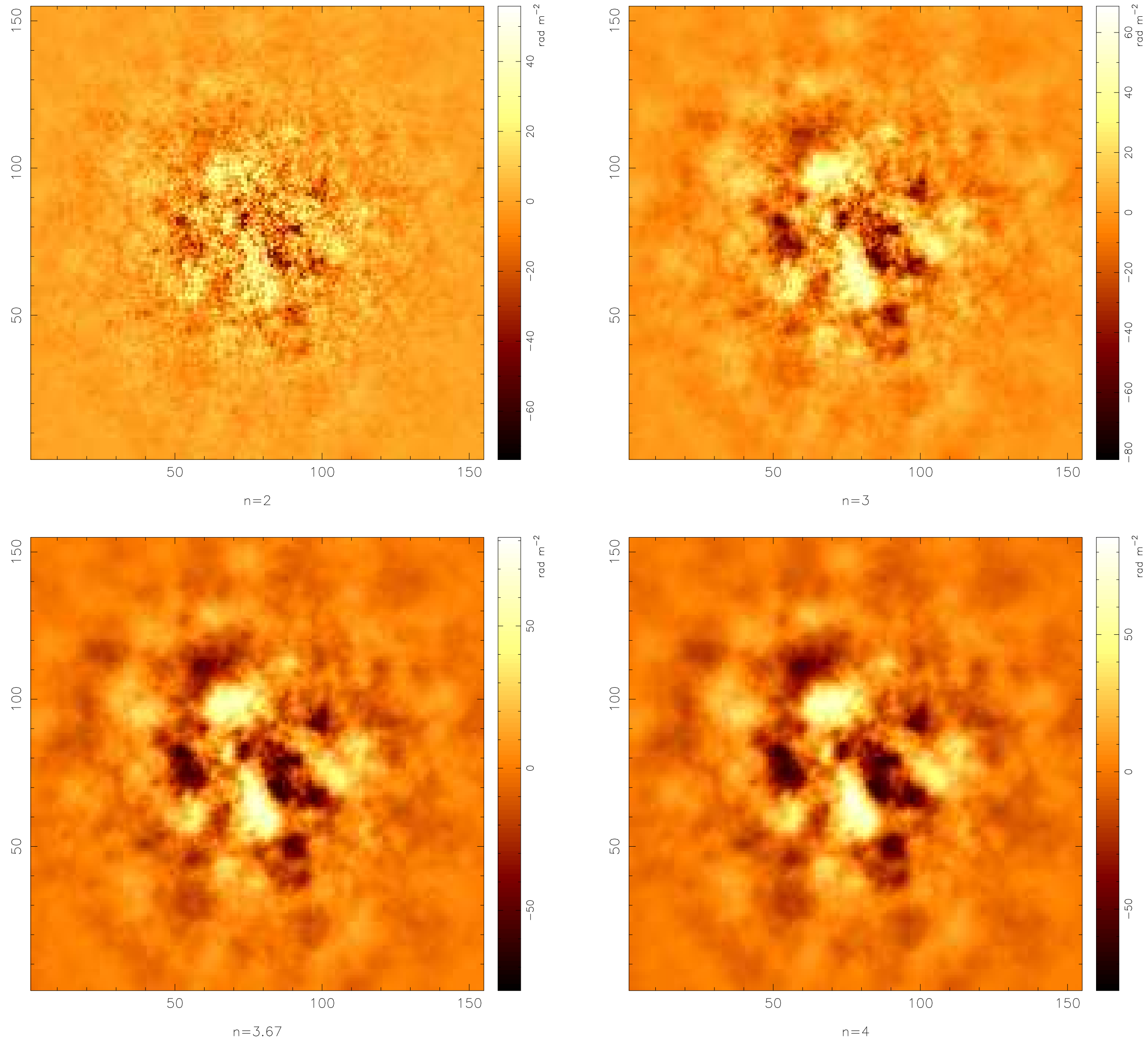

Fig. 5. Simulated RM images of a medium mass medium redshift galaxy cluster for different values of the spectral index of the power spectrum of magnetic field fluctuations.

Monte Carlo method (MCMC) to explore the posterior distribution and to evaluate how well "Faraday properties" can be constrained by future SKA observations. Thereby, our analysis assumes that redshifts (of the astrophysical objects on the line-of-sight) are a priori known to some realistic degree of precision as achievable by present X-ray and optical/infra-red facilities respectively. In Figure 7 reconstruction uncertainties on the inferred polarisation angle and foreground screen RM are shown for a particular radio source model as function of its total radio flux. The constraints are obtained by marginalising in each case over all other parameters. In Figure 8 we plot two-dimensional confidence contours for constraints on the intrinsic polarisation angle of a common source and the RM value of the foreground screen region, which it illuminates. As our analysis demonstrates RM synthesis, when performed on multi-channel spectro-polarimetric radio data as obtainable from future SKA observations, is a powerful method in order to explore magnetic field structures along the line-of-sight to a background polarised source (Faraday tomography). Nevertheless, some prior information is necessary to disentangle different Faraday contributions. Our RM synthesis code surpasses standard implementations inso-

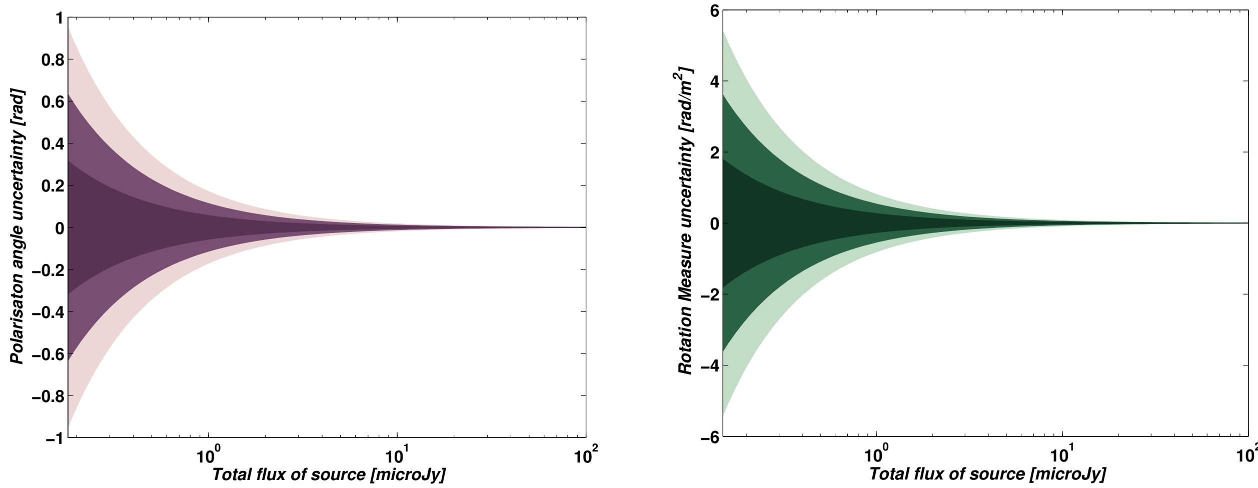

Fig. 7. Uncertainties on the reconstructed intrinsic source polarisation angle (left panel) and on the reconstructed RM of the foreground screen (right panel) for a single line-of-sight observation simulation as described in the text. In each case the different colour shading indicates the 1, 2 and 3σ uncertainty.

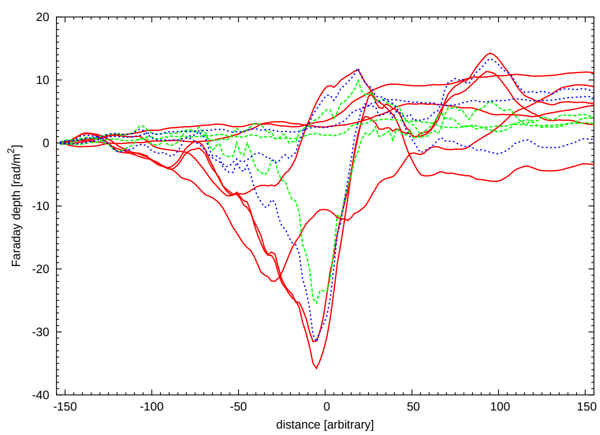

Fig. 6. Change of the Faraday depth for different lines of sight through the cluster. The colours and line-styles indicate different spectral indices of the cluster magnetic field power spectrum.

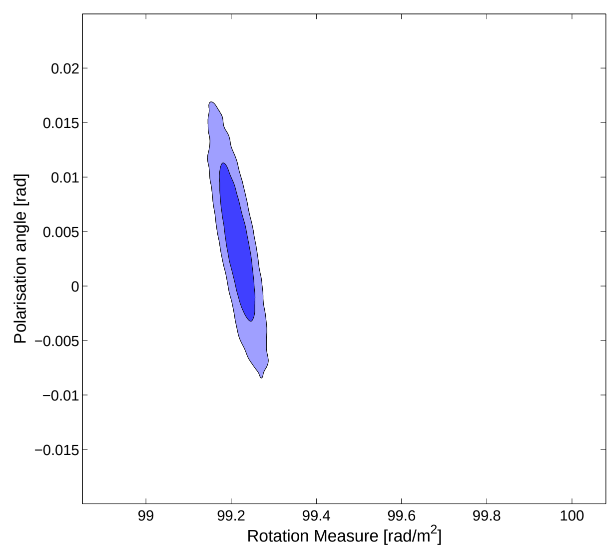

Fig. 8. Confidence limits for constraints on the foreground screen RM value and the intrinsic source polarisation angle. The dark blue shaded area gives the 68% and the light blue shaded one the 95% confidence region.

far that it applies Bayesian statistics and MCMC sampling of the posterior. These features are important due to their model selection and error estimation abilities for Faraday tomography. Furthermore, this code can be applied in RM as well as in frequency space. Latter has the advantage of avoiding a RM-cleaning which is otherwise due to bandwidth limitations often required in order to reduce noise correlations between discrete RM bins. The algorithm can in general be performed on cleaned image or $u-v$ data respectively.

6. CONCLUSIONS

Present studies of magnetic fields in the Universe are limited by the rather low resolutions and sensitivities achievable with present radio telescopes. In addition, due to hard- and software limitations, instantaneous bandwidth coverages and channel numbers are small. Therefore, only nearby galaxies and very low redshift clusters have been studied so far in a rather crude manner, e.g. RM grids are very sparsely meshed. There is little known about the evolution and the seeds of magnetic fields in the Universe (see e.g., Kronberg et al. 2008). However, our simulations imply that future SKA observations will be able to yield unmatched insights into the magnetic Universe. Already the SKA pathfinder instruments, which are namely the Low Frequency Array (LOFAR), the expanded Merlin (e-Merlin), the expanded Very Large Array (EVLA), the Murchison Widefield Array (MWA), the Long Wavelength Array (LWA), the Allen Telescope Array (ATA), the Karoo Array Telescope (MeerKAT) and the Australian SKA Pathfinder (ASKAP), will have the ability to significantly improve our knowledge of the magnetic Universe. Their different designs will allow us to study different aspects of cosmic magnetic fields. For instance, at low frequencies, at which LOFAR, MWA and LWA operate, outer galactic disks and halo fields of normal galaxies, deep spectrum cluster halos as well as cluster outskirts and the cosmic web can be probed. Moreover, also features of the Galactic magnetic field are still controversial (see e.g., Han 2008; Men et al. 2008; Sun et al. 2008) and need further investigations. In order to study (and possibly optimise) the usability of a telescope (here the SKA) for purposes of cosmic magnetic fields science, we obtain performance predictions from observation simulations based on various proposed (SKA) telescope designs and model realisations of the radio sky appearance in the observing band. Hence, we developed detailed polarised sky simulations on the basis of semi-empirically, analytically and numerically derived source models and assumed the latest published telescope specifications. Moreover, we implemented a Bayesian RM synthesis method which has been successfully tested on mock observations. Our implementation is, due to its model discrimination abilities based on Bayesian evidence selection, especially useful for Faraday tomography. Applications of this method to simulated data have succeeded in successfully separating Faraday structures under realistic prior assumptions.

REFERENCES

Alexander, P., Krause, M., Bolton, R., Riley, J., & Geisbuesch, J. 2008, in From Planets to Dark Energy: The Modern Radio Universe, Pos(MRU2007)068 (Trieste: SISSA)

Beck, R., Brandenburg, A., Moss, D., Shukurov, A., & Sokoloff, D. 1996, ARA&A, 34, 155

Condon, J., Cotton, W., Greisen, E., Yin, Q., Perley, R., Taylor, G., & Broderick J. 1998, AJ, 115, 1693

Geisbuesch, J., Alexander, P., Krause, M., & Bolton, R. 2008, N. Cim. B, 122, 1253

Han, J. 2008, IAU Symp. 242, Astrophysical Masers and their Environments, ed. J. M. Chapman & W. A. Baan (Cambridge: Cambridge Univ. Press), 55

Kronberg, P., Bernet, M., Miniati, F., Lilly, S., Short, M., Higdon, D., Taylor, G., & Dolag, K. 2008, ApJ, 676, 70

Men, H., Ferriere, K., & Han, J. 2008, A&A, 486, 819

Murgia, M., Govoni, F., Feretti, L., Giovannini, G., Dallacasa, D., Fanti, R., Taylor, G., & Dolag, K. 2004, A&A, 424, 429

Schilizzi, R., Alexander, P., Cordes, J., Dewdney, P., Ekers, R., Faulkner, A., Gaensler, B., Hall, J., Jonas, J., & Kellermann, K. 2007, SKA Memo 100 (Manchester: SPDO)

Sun, X., Reich, W., Waelkens, A., & Enßlin, T. 2003, A&A, 477, 573

Tucci, M., Martinez-Gonzalez, E., Toffolatti, L., Gonzalez-Nuevo, J., & de Zotti, G. 2003, NewA Rev., 47, 1135

Wilman, R., et al. 2008, MNRAS, 388, 1335